

Technical University of Denmark



Simulation of Nonlinear Gain Saturation in Active Photonic Crystal Waveguides

Chen, Yaohui; Mørk, Jesper

Published in:
International Conference on Photonics in Switching (PS)

Publication date:
2012

[Link back to DTU Orbit](#)

Citation (APA):
Chen, Y., & Mørk, J. (2012). Simulation of Nonlinear Gain Saturation in Active Photonic Crystal Waveguides. In International Conference on Photonics in Switching (PS) IEEE.

DTU Library
Technical Information Center of Denmark

General rights

Copyright and moral rights for the publications made accessible in the public portal are retained by the authors and/or other copyright owners and it is a condition of accessing publications that users recognise and abide by the legal requirements associated with these rights.

- Users may download and print one copy of any publication from the public portal for the purpose of private study or research.
- You may not further distribute the material or use it for any profit-making activity or commercial gain
- You may freely distribute the URL identifying the publication in the public portal

If you believe that this document breaches copyright please contact us providing details, and we will remove access to the work immediately and investigate your claim.

Simulation of Nonlinear Gain Saturation in Active Photonic Crystal Waveguides

Yaohui Chen and Jesper Mørk
 DTU Fotonik, Department of Photonics Engineering
 Technical University of Denmark
 Kgs. Lyngby, Denmark
 Yach@fotonik.dtu.dk

Abstract—In this paper we present a theoretical analysis of slow-light enhanced traveling wave amplification in an active semiconductor Photonic crystal waveguides. The impact of group index on nonlinear modal gain saturation is investigated.

Keywords—Photonic crystal waveguides; Semiconductor Optical Amplifier, Slow light, Gain saturation

I. INTRODUCTION

Photonic crystal (PhC) structures have been proposed as a potential waveguide infrastructure for high-density photonic integrated circuits (PICs). Optical amplification is one of the fundamental functionalities, required for compensating attenuation and coupling losses and thus increasing the number of integrated devices. A major advantage in combining PhC waveguides and active III-V semiconductors may be the possibility to drastically decrease the component length via enhanced light-matter interaction enabled by slow-light (SL) propagation [1]. The investigation of group velocity related gain enhancement was initiated in Bragg slabs [2]. It is natural to extend such idea to PhC line defect waveguides with guided modes within the bandgap [3]. Comparing with successful progresses of PhC Lasers [4], the attempts of realizing the PhC travelling wave semiconductor optical amplifiers (SOAs) [5] lead to various challenges, e.g. heating in membranes.

Instead of computational intensive 3-dimensional ab-initio simulations of Maxwell-Bloch equations [6], one-dimensional coupled-wave analysis based on a perturbative approach has been widely used to investigate the impact of SL effect on optical properties of passive PhC waveguides, e.g. Kerr nonlinearity [7,8] or disorder-induced scattering [9,10]. Meanwhile, the carrier dynamics of active semiconductor material can be well-described by macroscopic rate equation approaches [11]. However, so far, only a simple rate equation analysis [5] with heuristic inclusion of group velocity has been suggested to qualitatively investigate the gain characteristics of PhC travelling wave SOAs.

In this work, we present a theoretical analysis of SL-enhanced CW light amplification in active PhC membrane waveguides (as a travelling wave optical amplifier) as shown in Fig. 1. In particular, we focused on the carrier-depletion-induced modal gain saturation based on a rigorous carrier dynamics analysis.

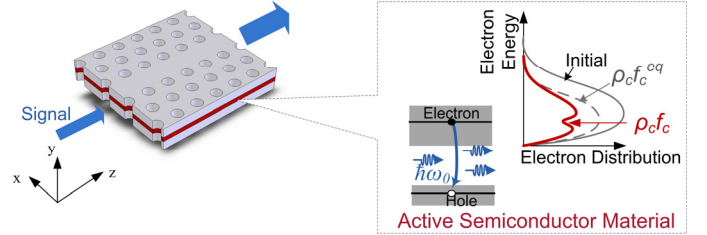


Fig. 1 Schematic illustration of active semiconductor photonic crystal waveguides as a travelling wave optical amplifier. ρ_c^{eq} and ρ_c are the corresponding quasi-equilibrium and non-equilibrium electron distributions in the presence of stimulated emission in the large-signal regime.

II. THEORY

In the weak perturbation limit, we approximate the exact solution of Maxwell equations as a monochromatic principal (i.e. TE-like) guided Bloch wave (obtained for the corresponding passive structure) with a forward amplitude $\psi(z)$ along propagation direction z . For simplicity, we only consider the carrier-induced imaginary susceptibility perturbation, as a product of an imaginary susceptibility constant χ_{pert} , an active material distribution function $F(r)$ and population inversion factor $f_c(r)+f_v(r)-1$. $f_\alpha(r)$ ($\alpha=c,v$) are the occupation probabilities in the conduction and valence band of semiconductor material. By using Lorentz reciprocity theorem, a propagation equation for the field amplitude [12] can be derived as:

$$\partial_z \psi(z) = \frac{i\omega}{c} n_{gz} \chi_{pert} \delta(z) \psi(z), \quad (1)$$

$$\delta(z) = \frac{a}{4W} \int_S \epsilon_0 |\mathbf{e}|^2 F(r) [f_c(r) + f_v(r) - 1] dS,$$

$$P_z = \frac{1}{2} \int_S \text{Re} \{ \mathbf{e} \times \mathbf{h}^* \} \cdot \hat{\mathbf{z}} dS, \quad W = \frac{1}{4} \int_V [\epsilon_0 n_b^2(r) |\mathbf{e}|^2 + \mu_0 |\mathbf{h}|^2] dV = \frac{an_{gz}}{c} P_z$$

Here \mathbf{e} , \mathbf{h} are the electric and magnetic fields of the periodic Bloch mode at frequency ω with propagation constant β . S indicates the transverse plane at position z , a is the lattice constant, V is the volume of a supercell, c is the speed of light in vacuum, n_{gz} is the group index along the waveguiding direction z . ϵ_0 , μ_0 are the electric and magnetic permittivities of free space. $n_b(r)$ is the background index. W is the unit rms electric and magnetic stored energy in a supercell, which is related to the unit rms power flux P_z over the transverse section by the Lorentz reciprocity theorem. $\delta(z)$ is propagation coefficient induced by the perturbation due to the active material. We define the carrier-induced material gain as

$g_{mat}=g_0(f_c+f_v-1)$, where the maximum material gain is $g_0=2n_{i0}\omega/c$. The corresponding imaginary refractive index n_{i0} and imaginary susceptibility constant $\chi_{peri}=-i2n_b n_{i0}$. By neglecting variation of field envelope within a supercell and imposing spatial averaging of propagation coefficient, i.e., zero-order Fourier coefficient, Eq. (1) is equivalent to the one-dimensional propagation equations previously used for studying SL enhancement of gain/absorption [3, 5] in small-signal regime. Our approach also permits the inclusion of different loss mechanisms [9,10].

The corresponding occupation factor $f_\alpha(r,t)$ and total carrier density $N_\alpha(r,t)$ in the conduction and valence band ($\alpha=c,v$) of active semiconductor material are determined by the following distributed rate equations:

$$\begin{cases} F(r)\rho_\alpha\partial_t f_\alpha(r,t) = -R_{stim} + R_{rel,\alpha}, \\ F(r)\partial_t N_\alpha(r,t) = -R_{stim} + R_{pump} - F(r)N_\alpha/\tau_s, \end{cases} \quad \alpha = c,v \quad (2)$$

Here ρ_α is the local carrier density. τ_s is the carrier lifetime of total carrier density. R_{pump} is the injection rate of carriers by optical/electrical pumping. Stimulated emission rate R_{stim} and ultrafast carrier relaxation term $R_{rel,\alpha}$ are defined as follow:

$$R_{stim} = -\frac{1}{\hbar\omega} \frac{2\omega}{c} n_{gz} \text{Im}\{\chi_{peri}\} \xi(r) |\psi(z)|^2 P_z, \quad (3)$$

$$R_{rel,\alpha} = \rho_\alpha \frac{f_\alpha^{eq} - f_\alpha}{\tau_{rel,\alpha}} F(r), \quad \xi(r) = \frac{a}{4W} \varepsilon_0 |\mathbf{e}|^2 F(r) [f_c(r) + f_v(r) - 1],$$

Here \hbar is Planck's constant. Time constant $\tau_{rel,\alpha}$ describes ultrafast carrier-carrier scattering, which contributes to gain as spectral hole-burning (SHB) effects. f_α^{eq} is the quasi-equilibrium occupation factor. $\xi(r)$ is a normalization factor for the change rate of electron-hole pairs due to stimulated emission. The active material distribution function on both sides of equation is used to keep the conservation of carrier and photon numbers. Thus based on the same principle of conservation, the confinement factors used for the stimulated emissions in effective rate equations analysis [5] should be carefully customized for each PhC waveguide design. Severe spatial carrier depletions within PhC waveguides due to SL-enhanced stimulated emission are expected, which quantitatively depend on the details of carrier dynamics as well as PhC waveguide geometry and carrier transport properties [13].

We use Eq. (2) to directly calculate spatial carrier distribution within a supercell depleted by a guided Bloch mode with a given CW power flux level $P_{in}=|\psi|^2 P_z$. Then effective population inversion factors in quasi-equilibrium f_{inv} and non-equilibrium f_{inv}^{eq} are evaluated to facilitate the coupled-wave analysis by Eq. (1):

$$f_{inv} = \frac{\int_V |\mathbf{e}|^2 F(r) [f_c(r) + f_v(r) - 1] dV}{\int_V |\mathbf{e}|^2 F(r) dV}, \quad f_{inv}^{eq} = \frac{\int_V |\mathbf{e}|^2 F(r) [f_c^{eq}(r) + f_v^{eq}(r) - 1] dV}{\int_V |\mathbf{e}|^2 F(r) dV} \quad (4)$$

Thus the effective modal gain averaged within a supercell can be obtained:

$$g_{mod}(P_{in}) = g_0 \cdot 2n_b n_{gz} \cdot f_{inv} \cdot \frac{1}{4W} \int_V \varepsilon_0 |\mathbf{e}|^2 F(r) dV \quad (5)$$

Furthermore, semi-analytical formulas can be approximated to evaluate 1D propagation effects by Eq. (1):

$$f_{inv}^{eq} \approx f_{inv,0}^{eq} / (1 + P_{in}/P_{sat}), \quad f_{inv} = f_{inv}^{eq} / (1 + \varepsilon_{SHB} P_{in}) \quad (6)$$

TABLE I. SIMULATION PARAMETERS

$n_b^2=11.19$	$a=340\text{nm}$	$n_{i0}=0.006$
$\tau_s=1\text{ns}$	$\tau_{rel,\alpha}=70\text{fs}$	
air hole radius 0.26a	Single QW vertical confinement 8/290	

Here a nonlinear gain suppression factor ε_{SHB} in unit of $[\text{W}^{-1}]$ and saturation power P_{sat} are extracted to characterize the saturation contributions from ultrafast carrier-carrier scattering as well as total carrier density depletion.

The simulation examples and results presented in the paper were obtained in 2D using commercial finite element method (FEM) software COMSOL. For simplicity, we used W1 PhC waveguides with a single quantum well (QW), which is described by free carrier gain model [14] only considering electron distribution and homogenous carrier pumping over PhC waveguides. Typical simulation parameters are given in Table 1. In this case imaginary index perturbation $n_{i0}=0.006$ corresponds to a material gain $g_0=486\text{cm}^{-1}$ (full population inversion) at the wavelength of 1550nm.

III. RESULTS

A. Modal Gain in Small-signal Regime

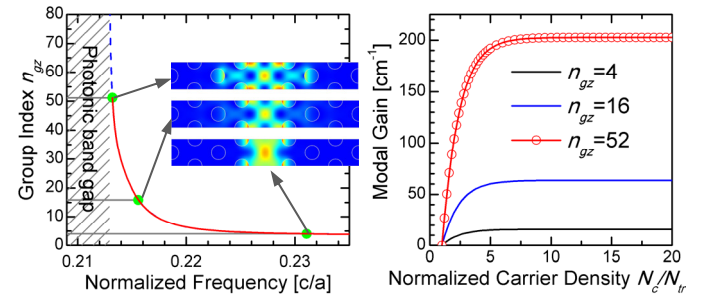


Fig. 2 SL enhancement of modal gain in active PhC waveguides in small-signal regime. (left) Group index as a function of normalized frequency. inset: 2D electric field intensity $|\mathbf{e}|^2$ as a function of group index. ($n_{gz}=4,16,52$) (right) Estimated modal gain in active PhC with different group index as a function of carrier density N_c (normalized by transparency density N_{tr}).

Fig. 2 illustrates the effective modal gain in active PhC W1 waveguides in the small-signal regime, which is determined by Eq. (5). Fig.2 (left) shows the calculated group index based on FEM eigen-frequency calculation of a 2D supercell. Due to different loss mechanisms in practical SL PhC waveguides [9,10] and fundamental limitations to gain enhancement close to photonic bandgap [15], we limit our discussions to slow light modes with group index up to around 50 and relative small imaginary refractive index change. The inset shows different electric field intensity distribution $|\mathbf{e}|^2$ as a function of group index, which will determine the strength of light-matter interaction and carrier depletion in Eq. (1)&(2).

As the carrier density in the active material increases beyond the transparency value N_{tr} , positive modal gain might be achieved to compensate propagation loss. Fig. 2(right) shows that the estimated maxima linear modal gain can be increased from $\sim 15\text{cm}^{-1}$ to 200cm^{-1} as group index increased from 4 to 52. The device length to realize a linear optical booster is considerably decreased. However, the corresponding SL enhanced differential gain also leads to modal gain saturation at lower input power.

B. Modal Gain in Large-signal Regime

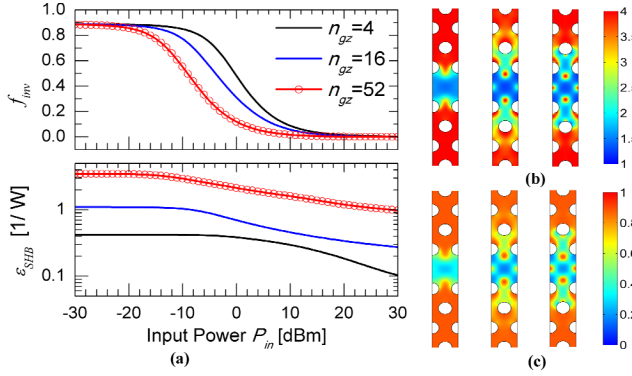


Fig.3 Impact of group index on CW modal gain saturation of active PhC waveguides. (a) Effective population inversion factor f_{inv} and corresponding nonlinear gain suppression factor ϵ_{SHB} as a function of input power P_m . Examples of (b) carrier density N_c (normalized by transparency density N_{tr}) and (c) population inversion factor f_{inv} when effective modal gains are halved in a supercell. From left to right: $n_{gz}=4, 16, 52$.

Fig. 3 shows examples of CW modal gain saturation for active PhC waveguides for different group index. As shown in Fig.3(a), when the input power increases, the effective population inversion f_{inv} declines toward zero. The saturation power of slow-light mode is lower than the one of the fast light mode due to the SL-enhanced stimulated emission. The slow-light mode has significantly higher gain suppression factor ϵ_{SHB} than the fast-light mode. This is mainly due to the fact that slow-light mode has higher electric field intensity than fast-light mode with a given input power. For the given parameters, the saturation power of slow-light mode ($n_{gz}=52$), which also limits the saturation output power of overall PhC SOAs, is around -10dBm. Fig.3(b)&(c) shows examples of carrier density distribution and population inversion factor when the effective modal gains are halved in a supercell. The patterns of carrier density and population inversion factor are related to the electric field intensity as shown in the inset of Fig. 2(left).

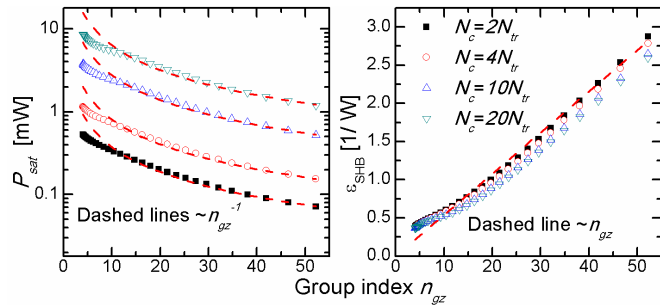


Fig. 4 Calculated saturation power P_{sat} and the corresponding nonlinear gain suppression factor ϵ_{SHB} as a function of group index with different initial carrier densities N_c normalized to transparency density N_{tr} . Dashed lines are fitting curves with dependence on group index.

By expanding Eq. (6) and keeping only the first two terms, we might find a nonlinear response proportional to ϵ_{SHB} and P_{sat}^{-1} , which contributes to an effective third-order susceptibility term with extra implicit dependence on group index in propagation equation Eq. (1). Fig. 4 shows the calculated saturation power and gain suppression factor as a

function of group index. The dashed lines are fitting curves to indicate that both ϵ_{SHB} and P_{sat}^{-1} roughly increase linearly as a function of group index despite deviations in the fast light region. Similar to Kerr nonlinearity [7], the large carrier-induced third-order susceptibility in active PhC waveguides might be also roughly scaled up with n_{gz}^2 . Considering the lower saturation power, PhC SOAs with SL enhancement is more attractive for nonlinear signal processing, e.g. Four-wave mixing (FWM), rather than linear optical amplification [5].

IV. CONCLUSION

We presented a theoretical investigation of CW modal gain saturation in active PhC waveguides with a set of rigorously derived carrier dynamics and couple-wave equations. Simulation indicates that SL-enhanced PhC SOAs as a travelling wave amplifier has higher peak modal gain at the expense of lower saturation power. The corresponding carrier-induced third-order susceptibility might be roughly scaled up quadratically with group index, which make active PhC waveguides potentially promising for nonlinear optical signal processing.

- [1] T. Baba, Slow light in photonic crystals, *Nature Photonics*, 2, 465-473, 2008
- [2] J. P. Dowling, M. Scalora, M.J. Bloemer and C.M. Bowden, The photonic band edge laser: A new approach to gain enhancement, *J. Appl. Phys.* 75, 1896-1899, 1994
- [3] J. Mørk and T.R. Nielsen, On the use of slow light for enhancing waveguide properties, *Opt. Lett.* 35, 2834-2836, 2010
- [4] S. Matsuo et al., High-speed ultracompact buried heterostructure photonic-crystal laser with 13 fJ of energy consumed per bit transmitted, *Nature Photonics*, 4, 648-654, 2010
- [5] E. Mizuta, H. Watanabe and T. Baba, All semiconductor low- Δ Photonic crystal waveguide for semiconductor optical amplifier, *Japan. J. Appl. Phys.*, 45, 6116, 2006
- [6] P. Bermel, E. Lidorikis, Y. Fink and J.D. Joannopoulos, Active materials embedded in photonic crystals and coupled to electromagnetic radiation, *Phys. Rev. B* 73, 165125, 2006
- [7] J.E. Sipe, N.A.R. Bhat, P.Chak, S. Pereira, Effective field theory for the nonlinear optical properties of photonic crystals, *Phys. Rev. E*, 69, 016604, 2004
- [8] N. C. Panoui, J.F. Mcmillan and C.W. Wong, Theoretical analysis of pulse dynamics in silicon photonic crystal wire waveguides, *IEEE J. Sel. Top. Quantum Electron.*, 16, 257-266, 2010
- [9] M. Patterson, et al., Disorder-induced incoherent scattering losses in photonic crystal waveguides: Bloch mode reshaping, multiple scattering, and breakdown of the beer-lambert, law *Phys. Rev. B*, 80, 195305, 2009
- [10] L. O'Faolain et al., Loss engineering slow light waveguides, *Opt. Express*, 18, 27627-27638, 2010
- [11] J. Mørk, A. Mecozzi, Theory of the ultrafast optical response of active semiconductor waveguides, *J. Opt. Soc. Am. B*, 13, 1803-1816, 1996
- [12] Y. Chen, F. Wang, S. Ek, J.S. Jensen, O. Sigmund and J. Mørk, Modeling of Gain Saturation Effects in Active Semiconductor Photonic Crystal Waveguides, *13th Intl. Conf. on Transparent optical Network (ICTON)*, 2011, paper We. C4.1
- [13] T. Tanabe, H. Taniyama and M. Notomi, Carrier diffusion and recombination in photonic crystal nanocavity optical switches, *J. Lightw. Technol.*, 26, 1396-1403, 2008
- [14] W. W. Chow, S.W. Koch, M. Sargent III, *Semiconductor-Laser Physics*, Springer-Verlag, 1994
- [15] J. Grgić et al., Fundamental limitations to gain enhancement in periodic media and waveguides, *Phys. Rev. Lett.*, 108, 183903, 2012